LETTERS

Climate-driven trends in contemporary ocean productivity

Michael J. Behrenfeld[1], Robert T. O'Malley[1], David A. Siegel[3], Charles R. McClain[4], Jorge L. Sarmiento[5], Gene C. Feldman[4], Allen J. Milligan[1], Paul G. Falkowski[6], Ricardo M. Letelier[2] & Emmanuel S. Boss[7]

Contributing roughly half of the biosphere's net primary production (NPP)[1,2], photosynthesis by oceanic phytoplankton is a vital link in the cycling of carbon between living and inorganic stocks. Each day, more than a hundred million tons of carbon in the form of CO_2 are fixed into organic material by these ubiquitous, microscopic plants of the upper ocean, and each day a similar amount of organic carbon is transferred into marine ecosystems by sinking and grazing. The distribution of phytoplankton biomass and NPP is defined by the availability of light and nutrients (nitrogen, phosphate, iron). These growth-limiting factors are in turn regulated by physical processes of ocean circulation, mixed-layer dynamics, upwelling, atmospheric dust deposition, and the solar cycle. Satellite measurements of ocean colour provide a means of quantifying ocean productivity on a global scale and linking its variability to environmental factors. Here we describe global ocean NPP changes detected from space over the past decade. The period is dominated by an initial increase in NPP of 1,930 teragrams of carbon a year ($Tg\,C\,yr^{-1}$), followed by a prolonged decrease averaging 190 $Tg\,C\,yr^{-1}$. These trends are driven by changes occurring in the expansive stratified low-latitude oceans and are tightly coupled to coincident climate variability. This link between the physical environment and ocean biology functions through changes in upper-ocean temperature and stratification, which influence the availability of nutrients for phytoplankton growth. The observed reductions in ocean productivity during the recent post-1999 warming period provide insight on how future climate change can alter marine food webs.

Interannual changes in phytoplankton abundance are small relative to total standing stocks and require accurate, long-term measurements to detect. The first satellite sensor to have this capability is the Sea-viewing Wide Field-of-View Sensor (SeaWiFS) and so far it is the only ocean colour sensor to have lunar-viewing calibration capabilities[3]. These measurements allow SeaWiFS to achieve water-leaving radiance biases across the SeaWiFS visible bands (412–555 nm) of less than 4% when compared to field open-ocean observations[4]. The central biological variable derived from these measurements is upper-ocean chlorophyll concentration, which can be used to estimate phytoplankton standing stocks and productivity (Fig. 1a) throughout the photic zone[5].

Global, depth-integrated chlorophyll biomass (ΣChl) for the 1997 to 2006 SeaWiFS record varied from 4.2 to 5.0 Tg ($Tg = 10^{12}$ g). Monthly anomalies in global ΣChl for this period reveal two highly significant ($P < 0.0001$) trends (green line in Fig. 1b). The initial 0.3 Tg rise in ΣChl corresponds to the 1997 to 1999 El Niño to La Niña transition[2]. Since 1999, global chlorophyll concentrations dropped on average 0.01 Tg per year, with several secondary features that ended in a 2005 to 2006 rise (Fig. 1b). The two primary trends in global ΣChl are driven by changes occurring in the permanently stratified regions of the ocean (grey circles in Fig. 1b). These regions have annual average sea surface temperatures (SSTs) over 15 °C (black lines in Fig. 1a) and represent 74% of the global ice-free ocean. Cooler, seasonal seas also experienced local variability during the SeaWiFS period, but when integrated spatially they exhibit no significant overall trend ($P > 0.5$) (Supplementary Fig. 1).

The entire phytoplankton biomass of the global oceans is consumed every two to six days[6]. This rapid turnover implies that variability in ΣChl (Fig. 1b) corresponds to far more substantial changes in NPP. One of the most commonly used models for estimating NPP from satellite chlorophyll data is the Vertically Generalized Production Model (VGPM)[6]. The VGPM gives global NPP estimates for the SeaWiFS record that vary strongly with season and range from 3.8 to 4.6×10^{15} g of C per month. Monthly anomalies in this important carbon flux again reveal clear ($P < 0.0001$) temporal trends beginning with an El Niño/La Niña-driven 262 Tg increase in NPP between 1997 and 1999, followed by a 197 Tg decrease to 2004, and finally a modest increase during 2005 (green line in Fig. 1c). These prominent NPP trends are again traceable to changes in the permanently stratified oceans (grey circles in Fig. 1c), are highly correlated ($r^2 = 0.93$) with changes in ΣChl (Fig. 1b), and remain when NPP is reassessed using alternative productivity models (Supplementary Fig. 2).

Perhaps the most challenging aspect of understanding variability in biological processes is associating detected changes with the environmental forcings responsible. Important climate variables linked to ocean circulation and productivity are sea-level pressure, surface winds, SST, surface air temperature, and cloudiness. These physical factors have been combined into a Multivariate ENSO Index (MEI) for evaluating the strength of El Niño/Southern Oscillation cycles[7,8]. Strong El Niño/Southern Oscillation events have major impacts on phytoplankton, fisheries, marine birds and mammals[2,9–12] and are striking examples of climatic influences on ocean biology. Importantly, the MEI does not distinguish between natural and anthropogenic changes in climate forcing, but instead provides an integrated index of climate conditions for comparison with observed changes in ocean productivity.

We find a clear, strong correspondence between MEI variability and SeaWiFS-based anomalies in NPP ($r^2 = 0.77$, $P < 0.005$) (Fig. 2a) and ΣChl (Supplementary Fig. 3). An increase in the MEI (that is, warmer conditions) results in a decrease in NPP and ΣChl, and vice versa. This relationship emphasizes the pre-eminent role of climate

[1]Department of Botany and Plant Pathology, 2082 Cordley Hall, and [2]College of Oceanographic and Atmospheric Sciences, Oregon State University, Corvallis, Oregon 97331, USA. [3]Institute for Computational Earth System Science and Department of Geography, University of California, Santa Barbara, Santa Barbara, California 93106-3060, USA. [4]NASA Goddard Space Flight Center, Greenbelt, Maryland 20771, USA. [5]Atmospheric and Oceanic Sciences Program, Princeton University, PO Box CN710, Princeton, New Jersey 08544, USA. [6]Environmental Biophysics and Molecular Ecology Program, Institute of Marine and Coastal Sciences and Department of Geological Sciences, Rutgers University 71 Dudley Rd, New Brunswick, New Jersey 08901, USA. [7]School of Marine Sciences, 209 Libby Hall, University of Maine, Orono, Maine 04469-5741, USA.

variability on ocean productivity trends. The observed physical–biological coupling between NPP and the MEI (Fig. 2a) functions through an effect of climate on water column stratification. Climatic changes that allow surface warming cause an increase in the density contrast between the surface layer and underlying nutrient-rich waters. For the global stratified oceans, the density difference between the surface and a depth of 200 m provides a useful measure of stratification. Monthly anomalies in this stratification index exhibit similar trends as the MEI for the SeaWiFS period (Fig. 2b). Importantly, enhanced stratification suppresses nutrient exchange through vertical mixing. Conversely, surface cooling favours elevated vertical exchange. Phytoplankton in the ocean's upper layer (that is, the populations observed from space) rely on vertical nutrient transport to sustain productivity, so intensified stratification during a rising MEI period (Fig. 2b) is accompanied closely by decreasing NPP (Fig. 2b) ($r^2 = 0.73$, $P < 0.005$).

The MEI captures global-scale trends in climate forcings on surface ocean growth conditions for phytoplankton (Fig. 2). However, while an increasing MEI corresponds to an overall warming period, at the regional scale both warming and cooling events are found. These regional changes are registered in satellite SST data and are well illustrated by the 1999 to 2004 period of increasing MEI. Comparison of SST changes (Fig. 3a) and modelled NPP changes (Fig. 3b) for this period reveals the anticipated inverse relationship of increasing temperatures coupled to decreasing production (Fig. 3c). Quantitatively, over 74% of the global oceans with SST changes exceeding $\pm 0.15\,^{\circ}C$ between 1999 and 2004 exhibited an inverse relationship between temperature and NPP changes (Fig. 3c). A consistent relationship is likewise observed between SST and ΣChl (Supplementary Fig. 4).

Our results clearly link ΣChl and NPP changes to SST, stratification and climate variations and provide an opportunity for comparison with simulated ocean responses to a warming climate. Atmosphere–ocean general circulation models coupled to ocean ecosystem models are essential tools for understanding global carbon cycle–climate feedbacks. When forced by rising atmospheric CO_2 concentrations, these prognostic models consistently yield increased SSTs and net decreases in stratified ocean NPP[13–16], consistent with observed changes in NPP during the 1999 to 2004 period of rising MEI (Fig. 2a). Also consistent with our results, model-simulated NPP changes are largely due to intensified water-column stratification and are not uniformly distributed across the stratified oceans[13–16]. A warming climate in atmosphere–ocean general circulation models is also generally associated with increased NPP at higher latitudes, owing to improved mixed-layer light conditions and extended growing seasons[14–16]. For our relatively brief observational record, this anticipated net increase in high-latitude NPP was not observed, although NPP changes were found regionally (Fig. 3b).

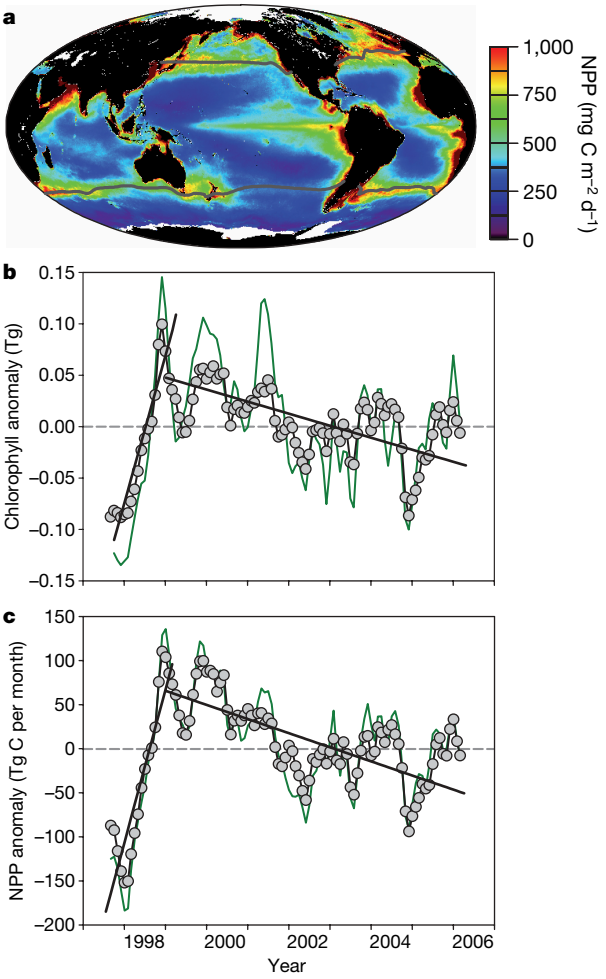

Figure 1 | Distribution and trends in global ocean phytoplankton productivity (NPP) and chlorophyll standing stocks. **a**, Annual average NPP showing high values where surface nutrients are elevated. Low-latitude, permanently stratified waters with annual average surface temperatures over 15 °C are delineated by black contour lines. **b**, Anomalies in globally integrated water-column chlorophyll concentrations (green line) are dominated by changes occurring in permanently stratified ocean regions (grey circles and black line). **c**, Anomalies in global NPP (green line) are likewise driven by changes in the permanently stratified oceans (grey circles and black line). Trend lines in **b** and **c** are least-squares fits to pre-1999 and post-1999 data.

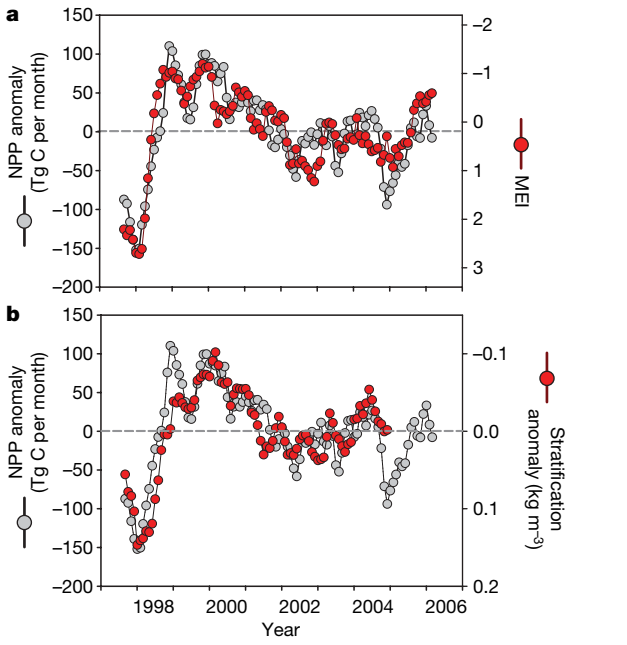

Figure 2 | Ocean productivity is closely coupled to climate variability. **a**, NPP anomalies in the permanently stratified oceans (grey symbols, left axis) are highly correlated ($r^2 = 0.77$) with the MEI of climate variability (red symbols, right axis). NPP data are from Fig. 1c. **b**, Changes in ocean stratification (red symbols, right axis) link climate variability to ocean biology, and are well correlated ($r^2 = 0.73$) with NPP anomalies (grey symbols, left axis) in ocean regions with annual average surface temperatures over 15 °C. Stratification strength was assessed as the density differences between the surface and a depth of 200 m using SODA data (see Methods). Publicly accessible SODA data are available only to the end of 2004. Note that the MEI and stratification axes (right) increase from top to bottom.

Establishing relationships between ocean biology and climate relies heavily on the accuracy to which changes in ocean ecosystems can be detected[3]. The unique operational characteristics of SeaWiFS have enabled detection of the global ocean trends reported here. Unfortunately, the SeaWiFS sensor is well beyond its design lifetime and no currently scheduled ocean-colour missions will have equal capabilities. SeaWiFS also represents an immature state of ocean-colour remote sensing. Modelling studies suggest that shifts in ecosystem structure from climate variations may be as or more important than the alterations in bulk integrated properties reported here[13]. Susceptible ecosystem characteristics include shifts in taxonomic composition[13], physiological status[17], and light absorption by coloured dissolved organic material[18]. Resolving these properties and their changes over time will require improved accuracies and significant expansions in the spectral range and resolution of future remote-sensing measurements.

Climate effects on ocean biology are documented here for nearly a decade of satellite ocean colour measurements. The compelling correspondence found between NPP changes and the MEI (Fig. 2a) suggests that this integrated index of climate variability, which extends back to 1950 (refs 6, 7), may provide a first-order proxy for variations in photosynthetic carbon fixation in the oceans for the period predating satellite ocean-colour measurements. It is also clear from the current analysis that surface warming in the permanently stratified ocean regions is accompanied by reductions in productivity. The index used here (MEI) to relate climate variability to NPP trends does not distinguish natural from anthropogenic contributions, but observational and modelling efforts indicate that recent changes in SST are strongly influenced by anthropogenic forcing[19–22]. These observations imply that the potential transition to permanent El Niño conditions in a warmer climate state[23] would lead to lower and redistributed ocean carbon fixation relative to typical contemporary conditions. Such changes will inevitably alter the magnitude and distribution of global ocean net air–sea CO_2 exchange[15,24,25], fishery yields[9,12,26], and dominant basin-scale biological regimes[12].

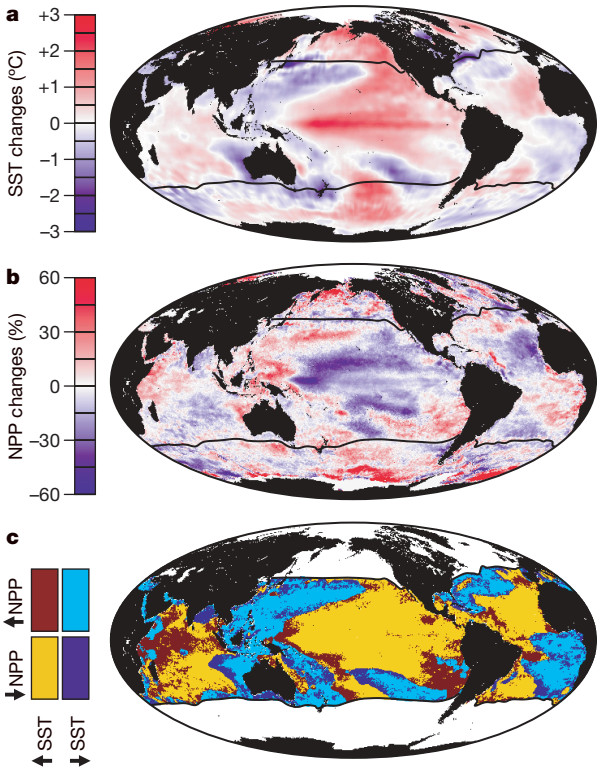

Figure 3 | Climate controls on ocean productivity cause NPP to vary inversely with changes in SST. Global changes in annual average SST (**a**) and NPP (**b**) for the 1999 to 2004 warming period (Fig. 2). **c**, For 74% of the permanently stratified oceans (that is, regions between black contour lines), NPP and SST changes were inversely related. Yellow, increase in SST, decrease in NPP. Light blue, decrease in SST, increase in NPP. Dark blue, decreases in SST and NPP. Dark red, increases in SST and NPP. A similar inverse relationship is observed between SST and chlorophyll changes. (See Supplementary Fig. 4 for additional information.)

METHODS

Ocean NPP was calculated with the VGPM using monthly 1,080 × 2,160 pixel resolution (that is, 18 km spacing at the Equator) OC4-v4 chlorophyll algorithm products from SeaWiFS reprocessed version 5.1 data (http://oceancolor.gsfc.nasa.gov). Comparison of this data with ~1,400 *in situ* match-up surface chlorophyll data yields a median difference of 33%, which is comparable to measurement uncertainties in the field. ΣChl was calculated from the satellite chlorophyll data using relationships described in ref. 5, which are based on 3,806 *in situ* chlorophyll profiles and account for subsurface chlorophyll features. The VGPM describes light-dependent changes in water-column NPP using a relationship based on 1,698 field productivity measurements[6] and SeaWiFS cloud-corrected photosynthetically active radiation data (http://oceancolor.gsfc.nasa.gov). The standard VGPM describes photosynthetic efficiencies using a polynomial function that increases with temperature below 20 °C and decreases above 20 °C.

Ocean NPP was additionally calculated using two alternative models, with results demonstrating the robust nature of the primary temporal trends described here (Supplementary Fig. 2). MEI data were from http://www.cdc.noaa.gov/people/klaus.wolter/MEI. Stratification anomalies were calculated from Simple Ocean Data Assimilation (SODA) (http://www.atmos.umd.edu/~ocean) monthly global density data, which assimilate available field observations. AVHRR SST data were from http://podaac-www.jpl.nasa.gov/sst. Deseasonalized chlorophyll, NPP, and stratification anomalies were calculated by subtracting from each monthly value the corresponding monthly average for the entire time series. Reported statistics for relationships between NPP anomalies and MEI and stratification anomalies account for auto-correlation effects inherent in comparisons between time-series data sets.

Received 18 August; accepted 6 October 2006.

1. Field, C. B., Behrenfeld, M. J., Randerson, J. T. & Falkowski, P. G. Primary production of the biosphere: Integrating terrestrial and oceanic components. *Science* **281,** 237–240 (1998).
2. Behrenfeld, M. J. *et al.* Biospheric primary production during an ENSO transition. *Science* **291,** 2594–2597 (2001).
3. McClain, C. R., Feldman, G. C. & Hooker, S. B. An overview of the SeaWiFS project and strategies for producing a climate research quality global ocean bio-optical time series. *Deep-Sea Res. II* **51,** 5–42 (2004).
4. Bailey, S. W. & Werdell, P. J. A multi-sensor approach for the on-orbit validation of ocean color satellite data products. *Remote Sens. Environ.* **102,** 12–23 (2006).
5. Morel, A. & Berthon, J-F. Surface pigments, algal biomass profiles, and potential production of the euphotic layer: relationships reinvestigated in view of remote-sensing applications. *Limnol. Oceanogr.* **34,** 1545–1562 (1989).
6. Behrenfeld, M. J. & Falkowski, P. G. Photosynthetic rates derived from satellite-based chlorophyll concentration. *Limnol. Oceanogr.* **42,** 1–20 (1997).
7. Wolter, K. The Southern Oscillation in surface circulation and climate over the tropical Atlantic, Eastern Pacific, and Indian Oceans as captured by cluster analysis. *J. Clim. Appl. Meteorol.* **26,** 540–558 (1987).
8. Wolter, K. & Timlin, M. S. Monitoring ENSO in COADS with a seasonally adjusted principal component index. In *Proc. 17th Climate Diagnostics Workshop (Norman, Oklahoma)* 52–57 (NOAA/N MC/CAC, NSSL, Oklahoma Climate Survey, CIMMS and the School of Meteorology, Univ. Oklahoma, 1993).
9. Barber, R. T. & Chavez, F. P. Biological consequences of El Niño. *Science* **222,** 1203–1210 (1983).
10. Chavez, F. P. *et al.* Biological and chemical response of the equatorial Pacific ocean to the 1997–98 El Niño. *Science* **286,** 2126–2131 (1999).
11. Turk, D., McPhaden, M. J., Lewis, M. R. & Busalacchi, A. J. Remotely-sensed biological production in the Tropical Pacific during 1992–1999. *Science* **293,** 471–474 (2001).
12. Chavez, F. P., Ryan, J., Lluch-Cota, S. E. & Niquen, M. C. From anchovies to sardines and back: Multidecadal change in the Pacific ocean. *Science* **299,** 217–221 (2003).
13. Boyd, P. W. & Doney, S. C. Modelling regional responses by marine pelagic ecosystems to global climate change. *Geophys. Res. Lett.* **29,** 1806, doi:10.1029/2001GL014130 (2002).
14. Bopp, L. *et al.* Potential impact of climate change on marine export production. *Glob. Biogeochem. Cycles* **15,** 81–99 (2001).
15. Le Quéré, C., Aumont, O., Monfray, P. & Orr, J. Propagation of climatic events on ocean stratification, marine biology, and CO2: Case studies over the

1979–1999 period. *J. Geophys. Res.* **108,** 3375, doi:10.1029/2001JC000920 (2003).
16. Sarmiento, J. L. *et al.* Response of ocean ecosystems to climate warming. *Glob. Biogeochem. Cycles* **18,** GB3003, doi:10.1029/2003GB002134 (2004).
17. Behrenfeld, M. J., Boss, E., Siegel, D. A. & Shea, D. M. Carbon-based ocean productivity and phytoplankton physiology from space. *Glob. Biogeochem. Cycles* **19,** GB1006, doi:10.1029/2004GB002299 (2005).
18. Siegel, D. A., Maritorena, S., Nelson, N. B. & Behrenfeld, M. J. Independence and interdependences of global ocean optical properties viewed using satellite color imagery. *J. Geophys. Res.* **110,** C07011, doi:10.1029/2004JC002527 (2005).
19. Levitus, S., Antonov, J. I., Boyer, T. P. & Stephens, C. Warming of the world ocean. *Science* **287,** 2225–2229 (2000).
20. Barnett, T. P., Pierce, D. W. & Schnur, R. Detection of anthropogenic climate change in the world's oceans. *Science* **292,** 270–274 (2001).
21. Levitus, S. *et al.* Anthropogenic warming of Earth's climate system. *Science* **292,** 267–270 (2001).
22. Barnett, T. P. *et al.* Penetration of human-induced warming into the world's oceans. *Science* **309,** 284–287 (2005).
23. Wara, M. W., Ravelo, A. C. & DeLaney, M. L. Permanent El Niño-like conditions during the Pliocene warm period. *Science* **309,** 758–761 (2005).
24. Sarmiento, J. L., Hughes, T. M. C., Stouffer, R. J. & Manabe, S. Simulated response of the ocean carbon cycle to anthropogenic climate warming. *Nature* **393,** 245–249 (1998).
25. Laws, E. A., Falkowski, P. G., Smith, W. O. Jr & McCarthy, J. J. Temperature effects on export production in the open ocean. *Glob. Biogeochem. Cycles* **14,** 1231–1246 (2000).
26. Ware, D. M. & Thomson, R. E. Bottom-up ecosystem trophic dynamics determine fish production in the Northeast Pacific. *Science* **308,** 1280–1284 (2005).

Supplementary Information is linked to the online version of the paper at www.nature.com/nature.

Acknowledgements We thank the Ocean Biology Processing Group at the Goddard Space Flight Center, Greenbelt, Maryland for their diligence in providing the highest quality ocean colour products possible and the NASA Ocean Biology and Biogeochemistry Program for support.

Author Information Reprints and permissions information is available at www.nature.com/reprints. The authors declare no competing financial interests. Correspondence and requests for materials should be addressed to M.J.B. (mjb@science.oregonstate.edu).